Physica D 238 (2009) 840–845

Contents lists available at ScienceDirect

Physica D

journal homepage: www.elsevier.com/locate/physd

New bisoliton solutions in dispersion managed systems

M. Shkarayev *, M.G. Stepanov

Department of Mathematics, The University of Arizona, 617 N. Santa Rita Ave., Tucson, AZ 85721, USA

ARTICLE INFO

Article history:
Received 29 November 2007
Received in revised form
2 December 2008
Accepted 2 February 2009
Available online 4 March 2009
Communicated by J. Bronski

Keywords:
Dispersion management
Bisoliton
Iterations convergence

ABSTRACT

In this paper we propose a method which provides a full description of solitary wave solutions of the Schrödinger equation with periodically varying dispersion. This method is based on analysis and polynomial deformation of the spectrum of an iterative map. Using this method we discover a new family of antisymmetric bisoliton solutions. In addition to the fact that these solutions are of interest for nonlinear fiber optics and the theory of nonlinear Schrödinger equations with periodic coefficients, they have potential applications for increasing of bit-rate in high speed optical fiber communications.
© 2009 Elsevier B.V. All rights reserved.

1. Introduction

Chromatic dispersion of optical fibers is one of the major factors limiting the capacity of fiber communication systems. It results in broadening of optical pulses due to differences in velocities of different spectral components. The dispersion management technique [1] was proposed as a method to solve the problem of dispersive pulse broadening. An optical fiber link with dispersion management is composed of periodically arranged fiber spans with alternating signs of dispersion. The fiber spans are chosen to make the cumulative effect of dispersion small or even zero. Full compensation of the dispersive effects is achieved by making the mean value of the dispersion to be zero. In this case as a pulse propagates over one period it will be spread and then contracted to its original shape.

Increasing bit-rates inevitably leads to manifestation of nonlinear properties of optical fibers. As bit rates increase, the temporal width of an optical pulse (bit carrier) τ_0 decreases. On the other hand the energy of the pulse must remain above some critical level $\mathcal{E} \geq \mathcal{E}_{\rm cr}$ to provide minimal detection bit-error at the end of the line, and therefore the power of the signal ($P \sim \mathcal{E}/\tau_0$) increases as the pulse narrows $P \geq \mathcal{E}_{\rm cr}/\tau_0$. It is a well known, experimentally verified fact that the index of refraction of the fiber core grows linearly with the power of the signal, $n = n_0 + \alpha P$ (where n_0 is linear index of refraction and α is a coefficient of Kerr nonlinearity). With a high enough power the nonlinear response of the medium becomes important. Since dispersion management is a purely linear approach to compensate for pulse broadening, the validity of this approach becomes less obvious in the presence of nonlinearity. It was shown that in presence of nonlinearity the compensation is still possible for a special class of pulses known as the dispersion managed (DM) solitons [2]. Detailed information about the DM solitons and their applications can be found in [3].

Soon after the concept of DM solitons was introduced, it became clear that both analytic representation and accurate numerical description of the DM soliton shape are challenging problems. The first problem was addressed in many papers, where approximations of the central part of the DM soliton and asymptotic of oscillatory tails was considered (see [4–6]). However the general solution of the this problem remains unsolved. The problem to determine an accurate numerical description of the DM soliton shape was solved by in [7–9] using a slow dynamics model of DM solitons proposed in [10]. Later this approach was used to address the behavior of DM solitons for the systems with both dispersion and nonlinearity compensation [11].

The dispersion compensation while resolving the physical problem with the pulse broadening, poses an obstacle for the numerical computation of such solutions. Following the standard approach, the description of a soliton consists of launching a signal and waiting for all the continuous radiation to escape. For the problem with dispersion management this process is extremely slow and ineffective on the tails of the soliton. Authors of [7] proposed solving the averaged equation for the analysis of solutions, which for the solitary waves reduces from an integro-differential equation to a nonlinear integral equation, solvable by a nonlinear iterative procedure. This allowed for a fast way of

* Corresponding address: Department of Mathematics, The University of Arizona, 617 N. Santa Rita Ave., P.O. Box 210089, Tucson, AZ 85721, USA. Tel.: +1 520 360 7871.

E-mail address: max@math.arizona.edu (M. Shkarayev).

0167-2789/$ – see front matter © 2009 Elsevier B.V. All rights reserved.
doi:10.1016/j.physd.2009.02.009

achieving precision exceeding any necessary requirements for the practical applications.

Unlike the conventional NLS soliton, the dispersion managed system supports propagation of bound pairs of solutions, or bisolitons. Existence of bisoliton solutions was shown in the numerical investigations of [12] and later confirmed experimentally in [13]. It should be noted that this experimental work considered antisymmetric bisolitons and therefore we limit our investigation to this type of bisoliton. These solutions are interesting for the theory of nonlinear partial differential equations, and represent a new phenomenon in nonlinear fiber optics. They illustrate a new type of solution of a nonlinear Schrödinger equation where the dispersion coefficient is replaced with a periodic function. The potential applications for the optical communication systems were discussed in [13]. Bisolitons can be used to introduce a three-letter alphabet ("empty slot", "DM soliton" and "bisoliton"), replacing a conventional binary alphabet. This could increase the system capacity without a change to the physical parameters of the system.

The shape as well as other important characteristics of bisolitons were found in [14] using a modification of the numerical method proposed in [7–9]. The equation describing averaged dynamics of the solution is reduced to have a single universal parameter, which incorporates all of the physical and geometrical characteristics of the optical system [14]. Analysis of this equation showed the existence of two branches of bisoliton determined by the universal parameter, with a critical bifurcation point connecting the two branches.

Investigation of DM bisolitons was based on the iteration of a nonlinear map. The analysis of the newly discovered branch of solutions was complicated by the lack of convergence of the iterative procedure. Careful analysis of the map showed the existence of eigenvalues outside of the unit circle, explaining the existence of the growing modes of the map. In this work we propose to utilize the method of polynomial spectral transformations to construct a contractive map, preserving the original fixed points. The application of this method allowed for the discovery of the previously unknown branch of bisoliton solutions. These bisolitons present new solutions to nonlinear Schrödinger equation with periodic dispersion. A recent paper [15] indicates new experimental evidence for the existence of this branch of bisoliton solutions. These newly found bisoliton solutions allow for the introduction of a 4-letter alphabet, further increasing the capacity of existing lines.

2. Basic equations

A well established model for the propagation of an electromagnetic pulse through a nonlinear, dispersive medium is the nonlinear Schrödinger equation

$$\mathrm{i}u_z + d(z)u_{tt} + \gamma|u|^2u = 0 \tag{1}$$

where the scalar function $u(z,t)$ is the envelope of the signal, z is the distance along the fiber, t is retarded time. Without loss of generality we consider a fiber link with constant nonlinearity given by γ. Function $d(z)$ is the dispersion as a function of distance along the fiber. For a dispersion managed system this is a piecewise constant, periodic function which can be written in the form $d(z) = d_0 + d_1$ if $0 < z < L/2$, and $d(z) = d_0 - d_1$ if $L/2 < z < L$, where L is a dispersion map period, and $d_1 \gg d_0$.

A fiber link with dispersion management has a characteristic time scale $\tau_{\mathrm{dm}} \equiv (Ld_1/2)^{1/2}$. The physical meaning of this time is the width of a pulse such that the pulse will approximately double in width as it propagates over half of the period. The characteristic "residual dispersion length" $z_{\mathrm{rd}} \equiv \tau_{\mathrm{dm}}^2/d_0 = Ld_1/2d_0$ is the distance when a pulse with width τ_{dm} propagating over a fiber with dispersion d_0 will approximately double in width. Rescaling the variables $t = \tau_{\mathrm{dm}}\tilde{t}$, $u = 2\pi\sqrt{P}\tilde{u}$ results in the equation

$$\mathrm{i}\tilde{u}_z + \frac{2}{L}\frac{d(z)-d_0}{d_1}\tilde{u}_{\tilde{t}\tilde{t}} + \frac{1}{z_{\mathrm{rd}}}\tilde{u}_{\tilde{t}\tilde{t}} + (2\pi)^2\frac{1}{z_{\mathrm{nl}}}|\tilde{u}|^2\tilde{u} = 0. \tag{2}$$

$z_{\mathrm{nl}} \equiv 1/(\gamma P)$ is characteristic "nonlinear length" on which the change of the phase of the pulse due to fiber nonlinearity will be of the order 1.

To take advantage of dispersion management in the presence of nonlinearity, the compensation must take place on the distances where nonlinearity effects are small and negligible compared to the local value of dispersion. Therefore the dispersion management works in the linear regime, and two well separated scales of pulse propagation can be distinguished. On the first scale local dispersion will dominate over the weak effects the residual dispersion and the nonlinearity. There the pulse is rapidly broadened and brought back to its original width as a result of the alternating signs of local dispersion. The second scale is where the effects of nonlinearity and residual dispersion accumulate and become important. Thus, the spectrum of the signal can be considered in the form

$$F[\tilde{u}] = q(\Omega, z)\exp\left(-\mathrm{i}\Omega^2/(L/2)\int_{L/4}^{z}\mathrm{d}\xi\,\frac{d(\xi)-d_0}{d_1}\right), \tag{3}$$

with the Fourier transform F defined as $F[f(t)] = \int \mathrm{d}t\, \exp(\mathrm{i}\omega t) f(t)$. Here the exponent is the rapidly changing phase due to the large value of local dispersion and the amplitude q is varying slowly with z due to residual dispersion and the nonlinear effects. Substituting this form of $\tilde{u}$ into the Eq. (2) and taking an average over a map period we obtain Gabitov–Turitsyn equation describing evolution of q [10]

$$\begin{aligned}
&\mathrm{i}q_z - \frac{1}{z_{\mathrm{rd}}}\Omega^2 q + \frac{1}{z_{\mathrm{nl}}}R(q,\Omega) = 0,\\
&R(q,\Omega) = \int \frac{\sin(\Delta/2)}{\Delta/2}q(\Omega_1)q(\Omega_2)q^*(\Omega_3)\\
&\qquad\times\delta(\Omega_1+\Omega_2-\Omega_3-\Omega)\mathrm{d}\Omega_1\mathrm{d}\Omega_2\mathrm{d}\Omega_3,
\end{aligned} \tag{4}$$

where $\Delta \equiv \Omega_1^2 + \Omega_2^2 - \Omega_3^2 - \Omega^2$, and $\delta(\cdot)$ is Dirac's delta function.

We are interested in computation of antisymmetric bisolitons which are solitary wave solutions of this equation. For such a solution the amplitude profile is independent of the distance along the fiber, and can be written as $q(\Omega,\tilde{z}) = \varphi(\Omega)\mathrm{e}^{\mathrm{i}\lambda\tilde{z}}$, where λ is a wave number of the solitary wave. With $\lambda = 1/z_{\mathrm{nl}}$ the function φ is governed by the following equation

$$\varphi + \bar{d}_0\Omega^2\varphi = R(\varphi,\Omega), \quad \text{where } \bar{d}_0 \equiv \frac{z_{\mathrm{nl}}}{z_{\mathrm{rd}}} = \frac{d_0}{(\gamma P)(d_1L/2)}. \tag{5}$$

Thus far we have reduced this three parameter partial differential equation to an integral equation with a single free parameter (an alternative way to do that is presented in Appendix A).

3. Solving the integral equation

In this paper we study the family of antisymmetric bisolitons at different positive values of parameter $\bar{d}_0$. In order to solve Eq. (5) we use the following iterative procedure [16]

$$\begin{aligned}
&\varphi_{n+1} = N_{\bar{d}_0}(\varphi_n), \qquad N_{\bar{d}_0}(\varphi) \equiv \mathbb{P}_{\mathrm{odd}}\left(Q^{3/4}\frac{R(\varphi,\Omega)}{1+\bar{d}_0\Omega^2}\right)\\
&Q \equiv \frac{\int|\varphi|^2\mathrm{d}\Omega}{\int\left|R(\varphi,\Omega)/\left(1+\bar{d}_0\Omega^2\right)\right|^2\mathrm{d}\Omega}
\end{aligned} \tag{6}$$

where Q is a Petviashvilli factor [17,18] which is introduced to avoid the convergence to the trivial solution $\varphi = 0$ by

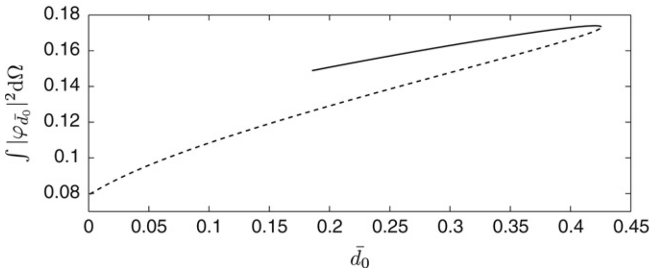

Fig. 1. Energy of the two branches of bisolitons as a function of $\bar{d}_0$. The solid line corresponds to the solutions with higher energy (upper branch) and the dashed line corresponds to solutions with lower energy (lower branch).

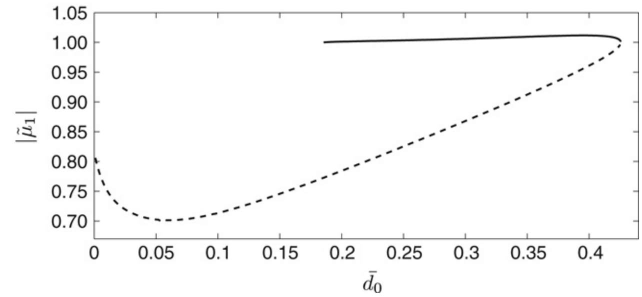

Fig. 2. A plot of largest eigenvalue of $\hat{K}$ as a function of time $\bar{d}_0$ at the upper branch solutions (solid) and at the lower branch solutions (dashed).

making that solution unstable. The operator $\mathbb{P}_{\mathrm{odd}}(f(\Omega)) \equiv (f(\Omega) - f(-\Omega))/2$ is a projection onto odd functions, used here to project the iterated functions onto the space of antisymmetric functions. We solve the Eq. (6) numerically, discretizing φ on a grid of M points. The iterations are stopped when φ_n satisfies the condition

$$\|\varphi_n + \bar{d}_0\Omega^2\varphi_n - R(\varphi_n, \Omega)\|_{L_2} < 10^{-8}. \tag{7}$$

A Fourier transform of a sum of two Gaussian pulses, shifted apart and taken with opposite signs is used as a seed for the iteration procedure with $\bar{d}_0 = 0.2$. The value of $\bar{d}_0$ is decreased incrementally, with a previous solution used as a seed for the next value of $\bar{d}_0$, until the parameter reaches zero. The same procedure was performed in the increasing direction from $\bar{d}_0 = 0.2$. We found two branches of bisoliton solutions. Fig. 1 shows the energy of the solutions as a function of $\bar{d}_0$. The solutions bifurcate near $\bar{d}_{0\mathrm{bf}} \approx 0.4256$. We observed no convergence for the values of $\bar{d}_0 > \bar{d}_{0\mathrm{bf}}$.

Direct application of the scheme in Eq. (6) demonstrates convergence only for the lower branch of solutions, and does not allow one to find the upper branch of solutions. In order to find the solutions from the upper branch we study the spectrum of the N and modify the map.

4. Convergence of the map *N*

In order to understand the convergence of the iterative procedure described in Eq. (6) we analyze the spectrum of $N_{\bar{d}_0}$ near a fixed point. In the neighborhood of the fixed point φ_{fp} the map $N_{\bar{d}_0}$ is approximated by the linear operator K:

$$N(\varphi_{\mathrm{fp}} + \Psi) = \varphi_{\mathrm{fp}} + K(\Psi) + \mathcal{O}(\Psi^2). \tag{8}$$

Here the operator K lacks the complex structure and should be viewed as a linear operator over the field of real numbers acting on a real vector space consisting of functions $\mathrm{Re}\,\Psi$ and $\mathrm{Im}\,\Psi$. Let the finite set $\{\mu_i\}$, $\{|\phi_i\rangle\}$, and $\{\langle\phi_i|\}$ correspond to eigenvalues, right eigenvectors and left eigenvectors of $\hat{K}$, the discretized version of K. Right away we see that there is an eigenvalue 1 corresponding to a constant phase shift of any fixed point. This eigenvector does not affect the convergence since Eq. (7) is unaffected by the constant phase shift. Therefore, we introduce the sets $\{\tilde{\mu}_i\} = \{\mu_i\} \setminus 1$ and $\{|\tilde{\phi}_i\rangle\} = \{|\phi_i\rangle\} \setminus |\phi_{\mu=1}\rangle$, $\{\langle\tilde{\phi}_i|\} = \{\langle\phi_i|\} \setminus \langle\phi_{\mu=1}|$ where we have removed the above eigenvector and the corresponding eigenvalue. Furthermore, we assume that if $i < j$ than $|\tilde{\mu}_i| \geq |\tilde{\mu}_j|$, so that $\tilde{\mu}_1$ has maximal magnitude. The following iterative procedure is used to obtain the Nth eigenfunction

$$|\tilde{\phi}_N\rangle = \lim_{n\to\infty} \Psi_n, \quad \text{where } \Psi_{n+1} = \frac{\hat{K}(\Psi_n) - \sum\limits_{j=1}^{N-1} \langle\tilde{\phi}_j|\hat{K}(\Psi_n)\rangle|\tilde{\phi}_j\rangle}{\int |\Psi_n|^2 \mathrm{d}\Omega} \tag{9}$$

where $\langle\tilde{\phi}_j|$ is a dual vector of $|\tilde{\phi}_j\rangle$, satisfying $\langle\tilde{\phi}_j|\tilde{\phi}_k\rangle = \delta_{jk}$ (here δ_{jk} is a Kronecker symbol). We assume here that initial function Ψ_0 has nonzero projection onto Nth eigenfunction. At each step of this procedure the largest $N-1$ modes are projected out of Ψ_n and in the limit as the number of iterations n goes to infinity the next largest mode is the only one that survives. The contribution from the Mth vector ($M > N$) dies out as $(\tilde{\mu}_M/\tilde{\mu}_N)^n$.

In order to perform the procedure described in Eq. (9) we use the explicit expression for the operator $\hat{K}$

$$\begin{aligned}
&\hat{K}(\Psi) = 1.5\varphi_{\mathrm{fp}} \int \mathrm{Re}\left[\varphi_{\mathrm{fp}}^*(\Psi - L(\Psi))\right] \mathrm{d}\Omega \Big/ \int |\varphi_{\mathrm{fp}}|^2 \mathrm{d}\Omega + L(\Psi) \\
&\text{and} \quad L(\Psi) \equiv \int \frac{\sin(\Delta/2)}{\Delta/2} \big(\varphi_{\mathrm{fp}}(\Omega_1)\varphi_{\mathrm{fp}}(\Omega_2)\Psi^*(\Omega_3) \\
&\quad + 2\varphi_{\mathrm{fp}}(\Omega_1)\Psi(\Omega_2)\varphi_{\mathrm{fp}}^*(\Omega_3)\big) \frac{\delta(\Omega_1 + \Omega_2 - \Omega_3 - \Omega)}{1 + \bar{d}_0\Omega^2} \mathrm{d}\bar{\Omega}
\end{aligned} \tag{10}$$

here $\mathrm{d}\bar{\Omega} = \mathrm{d}\Omega_1\mathrm{d}\Omega_2\mathrm{d}\Omega_3$. The operator $\hat{K}$ is not self-adjoint, therefore, its left and right eigenvectors are different. We obtain the the left eigenvectors of the operator $\hat{K}$ by studying the right eigenvectors of the operator $\hat{K}^\dagger$

$$\begin{aligned}
\hat{K}^\dagger(\xi) &= L^\dagger(\zeta) - \zeta + L^\dagger(\xi) \\
\zeta &\equiv 1.5\varphi_{\mathrm{fp}} \int \mathrm{Re}\left[\varphi_{\mathrm{fp}}^*\xi\right] \mathrm{d}\Omega \Big/ \int |\varphi_{\mathrm{fp}}|^2 \mathrm{d}\Omega \\
L^\dagger(\xi) &= \int \frac{\sin(\Delta_+/2)}{\Delta_+/2} \varphi_{\mathrm{fp}}(\Omega_1)\varphi_{\mathrm{fp}}(\Omega_2)\xi^*(\Omega_3) \\
&\quad \times \frac{\delta(\Omega_1 + \Omega_2 - \Omega_3 - \Omega)}{1 + \bar{d}_0\Omega_3^2} \mathrm{d}\bar{\Omega} \\
&\quad + \int \frac{\sin(\Delta_-/2)}{\Delta_-/2} 2\varphi_{\mathrm{fp}}(\Omega_1)\xi(\Omega_2)\varphi_{\mathrm{fp}}^*(\Omega_3) \\
&\quad \times \frac{\delta(\Omega_1 - \Omega_2 - \Omega_3 + \Omega)}{1 + \bar{d}_0\Omega_2^2} \mathrm{d}\bar{\Omega} \\
\Delta_\pm &\equiv \Omega_1^2 \pm \Omega_2^2 - \Omega_3^2 \mp \Omega^2.
\end{aligned} \tag{11}$$

Fig. 2 shows how the largest magnitude eigenvalue of the operator $\hat{K}$ depends on $\bar{d}_0$. Here the dashed line corresponds to the lower branch of solutions and the solid line corresponds to the upper branch of solutions. Since for all values of $\bar{d}_0$ the largest eigenvalue of $\hat{K}$ at the lower branch solutions is less than 1 the map N is contractive. Therefore as long as we are close enough to the fixed point the iterations will converge. The situation is different for the upper branch of solutions. As clearly shown on Fig. 3 for all values of $\bar{d}_0$ the largest eigenvalue is larger than 1 and therefore the map is not contractive.

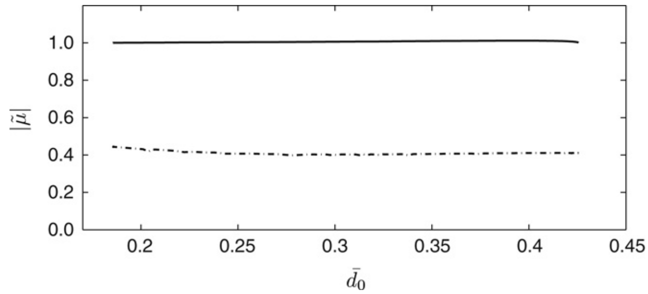

Fig. 5. A plot of $\tilde{\mu}_1$ (solid) and $\tilde{\mu}_2$ (dash-dot) versus $\bar{d}_0$. This plot indicated a large gap between the first two eigenvalues for the upper branch solutions.

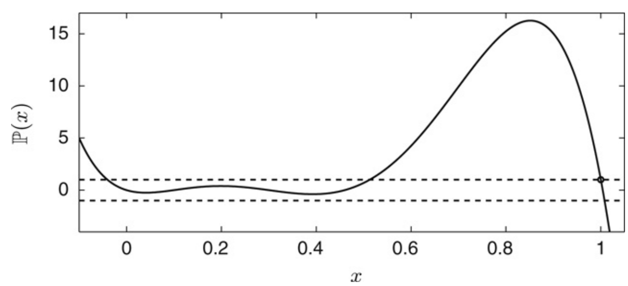

Fig. 6. This is a plot of a polynomial suggested in Eq. (15). Dashed lines indicate values of 1 and -1, outside of these values eigenvalues of $\mathbb{P}(N)$ will be greater than 1, in which case the new map will not be contractive.

(remember that $\bar{d}_0 \equiv d_0/(\gamma P)(d_1 L/2))$. Here F^{-1} is the inverse Fourier transform. The pulse is launched at $z = L/4$ because as Eq. (3) indicates at this point the phase of the solution $\varphi_{\bar{d}_0}$ is constant. Notice that parameters d_0, d_1, L and γ are determined by the physical system, while P is a free parameter whose value is limited from below due to the upper bound on $\bar{d}_0 = \bar{d}_{0\mathrm{bf}}$:

$$\frac{2d_0}{\bar{d}_{0\mathrm{bf}} d_1} \frac{1}{\gamma L} < P \ll \frac{1}{\gamma L}.$$

The inequality on the right must be maintained in order to stay in the regime where Gabitov–Turitsyn equation is valid. Fig. 7 shows the result of propagating u_0 over 3000 dispersion map periods. This distance exceeds the distances needed for information transmission. The solid line represents the initial pulse $u_0(t)$ of Eq. (16) launched at $z = L/4$. The pulse u_0 is constructed using a fixed point $\varphi_{\bar{d}_0=0.4}$ of the map $N_{\bar{d}_0=0.4}$. It is used as an initial condition for direct simulation of Eq. (1) solved using a split-step method. The dashed line shows an amplitude profile, plotted on a logarithmic scale, of the pulse after the distance $3000L$, showing excellent agreement between the initial and final pulses and confirming that $u_0(t)$ is indeed a good approximation to a solitary wave solution of Eq. (1).

7. Conclusion

In this paper we have presented a method to calculate solitary wave solutions of the nonlinear Schrödinger equation with periodic dispersion and weak nonlinearity. In case when the effect of local dispersion is much stronger than residual dispersion and nonlinearity the Schrödinger equation is reduced to Gabitov–Turitsyn equation, an integro-differential equation. This equation is satisfied by the first order term in the asymptotic expansion of a solution to the Schrödinger equation with periodic dispersion. Finding solitary wave solutions is then reduced to finding a solution of an integral equation by finding fixed points of a derived map.

We investigated bound pairs of solitary waves, bisolitons, and showed that system has at least two branches of nontrivial solutions. On one of these branches, our map is not contractive.

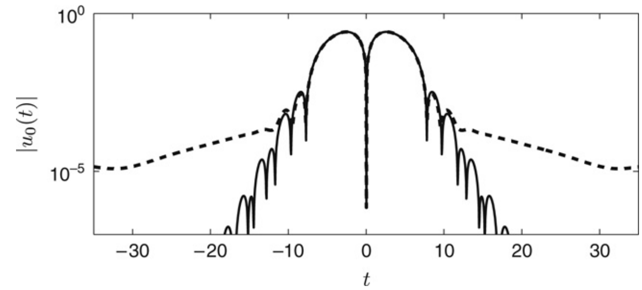

Fig. 7. Directly solving NLS equation with initial condition u_0 (solid) from Eq. (16) with lower branch solution $\varphi_{\bar{d}_0=0.214} d_0 = 0.0125$, $d_1 = 1.25$, $L = 1.2$ and $\gamma = 1$. The result of propagation u_0 over 3000 periods is represented by a dashed line, showing three orders of magnitude agreement between the initial and final pulses. Here $P \approx 0.0345$ so that $z_{\mathrm{rd}} = 45$ and $z_{\mathrm{nl}} = 29$.

We introduce a method to polynomially modify the map, obtaining a new map that retains the original fixed points, while being contractive. Effective use of this method resulted in a previously unknown branch of bisoliton solutions. In order to apply this method the spectrum of the map was studied. We carefully studied the parameter space where such solutions are possible, and found two places where solutions appear to bifurcate.

The method of polynomial deformation as applied to our problem can be further improved. The choice of the polynomials can be adapted as the knowledge about the spectrum improves in the process of iterations. Also, a better precision on the eigenvalues may allow one to further decrease the order of the polynomial, thus expediting the iteration procedure. The approach taken by this method is not limited to the antisymmetric solutions of our equation. Higher order solutions can be found after the appropriate modification of the map. Thus we have used this method to study symmetric bisolitons, with the results to be published elsewhere.

Authors would like to thank Ildar Gabitov and Linn Mollenauer for posing the problem, and Robert Indik and Sasha Korotkevich for the useful discussions during the work on this problem. This work supported in part by the State of Arizona grant TRIF (Proposition 301), NSFgrant EMSW21-VIGRE # 0602173, and by the Department of Energy at Los Alamos National Laboratory under contracts DE-AC52-06NA25396 and the DOE Office of Science Advanced Computing Research (ASCR) program in Applied Mathematical Sciences.

Appendix

Here we present another way of reducing the Eq. (1) to a dimensionless form. In the ω-space we introduce a slowly varying amplitude $q(z, \omega)$ as

$$u(z, \omega) = q(z, \omega) \exp\left(-\mathrm{i}\omega^2 \int_{L/4}^{z} \mathrm{d}z' \Big(d(z') - \langle d \rangle\Big)\right).$$

Here the angular brackets denote averaging over z. The slow (over many periods of the dispersion map) dynamics of q is described by the Gabitov–Turitsyn equation [10]

$$\mathrm{i}q_z(\omega) - \langle d \rangle \omega^2 q(\omega) + \gamma \int \frac{\mathrm{d}\omega_1 \mathrm{d}\omega_2 \mathrm{d}\omega_3}{(2\pi)^2}$$
$$\times\, \delta(\omega_1 + \omega_2 - \omega_3 - \omega) S(\delta) q(\omega_1) q(\omega_2) q^*(\omega_3) = 0,$$
$$\delta = \omega_1^2 + \omega_2^2 - \omega_3^2 - \omega^2,$$
$$S(\delta) = \left\langle \exp\left(-\mathrm{i}\delta \int_{L/4}^{z} \mathrm{d}z' \Big(d(z') - \langle d \rangle\Big)\right)\right\rangle.$$

For the dispersion map $d(z) = d_0 + d_1$ if $0 < z < L/2$, and $d(z) = d_0 - d_1$ if $L/2 < z < L$ we get $S(\delta) = \sin(\delta L d_1/4)/(\delta L d_1/4)$. We choose $\sqrt{L d_1/2}$ to be a unit of time and introduce the dimensionless frequency $\Omega = \sqrt{Ld_1/2}\omega$. Then $S(\Delta) = \sin(\Delta/2)/(\Delta/2)$, where $\Delta = \Omega_1^2 + \Omega_2^2 - \Omega_3^2 - \Omega^2$.

We set the residual dispersion to be equal to $1/2$ by choosing the unit of propagation distance: $Z = (4d_0/Ld_1)z$. The nonlinearity coefficient γ can be eliminated by choosing the unit of the pulse amplitude u (or q): $q(z,\omega) = \sqrt{2d_0/\gamma}\, Q(Z,\Omega)$.

The dimensionless form of the Gabitov–Turitsyn equation becomes

$$\mathrm{i}Q_Z(\Omega) - \frac{1}{2}\Omega^2 Q(\Omega) + \int \frac{\mathrm{d}\Omega_1\mathrm{d}\Omega_2\mathrm{d}\Omega_3}{(2\pi)^2} \times \delta(\Omega_1 + \Omega_2 - \Omega_3 - \Omega)\frac{\sin(\Delta/2)}{\Delta/2} Q(\Omega_1)Q(\Omega_2)Q^*(\Omega_3) = 0. \quad (17)$$

The stationary shape solutions have the form $Q(Z,\Omega) = \mathrm{e}^{\mathrm{i}\Lambda Z}\varphi(\Omega)$ — there is a family of solutions parameterized by wave number Λ.

The main point of this appendix is to present another way to bring the Eq. (1) to the dimensionless form. In the main part of the text the final step in reducing the number of parameters is done by choosing the inverse wave number of the solution as the unit of propagation distance. This way the only remaining parameter is the dimensionless residual dispersion $\bar{d}_0$ that is related to the wave number of the solution of (17) Λ as $\bar{d}_0 = 1/2\Lambda$. The advantage of this approach is that we now study the family of solutions of one Eq. (17) instead of considering a family of equations (parametrized by $\bar{d}_0$), where for each of these equations a solution is found with a certain wave number.

References

[1] C. Lin, H. Kogelnik, L.G. Cohen, Opt. Lett. 5 (1980) 476.
[2] F.M. Knox, W. Forysiak, N.J. Doran, J. Lightwave Technol. 13 (1995) 1955.
[3] L.F. Mollenauer, J.P. Gordon, Solitons in Optical Fibers: Fundamentals and Applications, Academic Press, New York, 2006.
[4] S. Kumar, A. Hasegawa, Opt. Lett. 22 (1997) 372.
[5] S.K. Turitsyn, V.K. Mezentsev, Dynamics of self-similar dispersion-managed soliton presented in the basis of chirped Gauss-Hermite functions, JETP Lett. 67 (9) (1998) 640–646.
[6] A.V. Mikhailov, V.Yu. Novokshenov, The period map for pulse propagation in nonlinear optical DM fibres, JETP Lett. 73 (5) (2001) 250–254.
[7] P.M. Lushnikov, Dispersion-managed soliton in optical fibers with zero average dispersion, Opt. Lett. 25 (16) (2000) 1144–1146.
[8] P.M. Lushnikov, On the boundary of the dispersion-managed soliton existence, JETP Lett. 72 (3) (2000) 111–114.
[9] P.M. Lushnikov, Dispersion-managed soliton in a strong dispersion map limit, Opt. Lett. 26 (20) (2001) 1535–1537.
[10] I. Gabitov, S.K. Turitsyn, Opt. Lett. 21 (1996) 327.
[11] I.R. Gabitov, P.M. Lushnikov, Nonlinearity management in dispersion managed system, Opt. Lett. 27 (2) (2002) 113–115.
[12] A. Maruta, T. Inoue, Y. Nonaka, Y. Yoshika, IEEE J. Sel. Top. Quantum Electron. 8 (2002) 640.
[13] M. Stratmann, T. Pagel, F. Mitschke, Phys. Rev. Lett. 95 (2005) 143902.
[14] I. Gabitov, R. Indik, L. Mollenauer, M. Shkarayev, M. Stepanov, P.M. Lushnikov, Twin families of bisolitons in dispersion-managed systems, Opt. Lett. 32 (6) (2007) 605–607.
[15] A. Hause, H. Hartwig, B. Seifert, H. Stolz, M. Böhm, F. Mitschke, Phys. Rev. A 75 (2007) 063836.
[16] P.M. Lushnikov, Opt. Lett. 26 (2001) 1535.
[17] V.I. Petviashvili, On the equation of an unusual soliton, Fiz. Plazmy 2 (3) (1976) 469–472 (in Russian).
[18] V. Petviashvili, O. Pokhotelov, Solitary Waves in Plasmas and in the Atmosphere, Gordon & Breach, Philadelphia, Pa, 1992, p. 248.
[19] A.I. Chernykh, M.G. Stepanov, Large negative velocity gradients in Burgers turbulence, Phys. Rev. E 64 (2001) 026306.
[20] A. Greenbaum, L.N. Trefethen, GMRES/CR and Arnoldi/Lanczos as matrix approximation problems, SIAM J. Sci. Comput. 15 (1994) 359–368.
[21] L.N. Trefethen, D. Bau, Numerical Linear Algebra, SIAM Press, Philadelphia, 1997.
[22] K.-C. Toh, L.N. Trefethen, The Chebyshev polynomials of a matrix, SIAM J. Matrix Anal. Appl. 20 (2) (1999) 400–419.